

Optimal tuning of robust proportional integral derivative based on sliding mode controller for an AVR system

Lemita Abdallah¹, Lemita Ines², Kahla Sami³

¹Department of Electrical Engineering, Faculty of Sciences and Technology, Echahid Cheikh Larbi Tebessi University, Tebessa, Algeria

²Department of Electrical Engineering, Faculty of Sciences and Technology, University of Mohamed Cherif Messaadia, Souk Ahras, Algeria

³Research Center in Industrial Technologies (CRTI), Cheraga, Algeria

Article Info

Article history:

Received Dec 8, 2024

Revised Jul 14, 2025

Accepted Jul 29, 2025

Keywords:

Automatic voltage regulator
Particle swarm optimization
Proportional integral derivative
controller

Robust control

Sliding mode control

ABSTRACT

The primary objective of the automated voltage regulator (AVR) is to maintain the terminal voltage of the synchronous generator at the specified level with great precision in power production systems. Accurate voltage regulation improves the longevity of equipment intended for operation at the specified voltage within a power system network. This study presents a robust control of an AVR system utilizing proportional integral derivative (PID) control based on sliding mode techniques. The suggested control method is implemented by utilizing the particle swarm optimization (PSO) technique to tune the parameters of the proposed controller in the AVR system. A comparative performance analysis is conducted between the proposed controller, PID controller, and (PSO-fractional order proportional integral derivative (FOPID) controller. The comparison is derived using transient response characteristics and parameter uncertainty. The results reveal that the proposed PSO-PID-sliding mode control (SMC) controller has superior performance, characterized by rapid convergence, reduced overshoot, stability achievements in time domains, and robustness against parameter fluctuations. The proposed controller has markedly enhanced the performance of the AVR system and can be effectively implemented inside it.

This is an open access article under the [CC BY-SA](https://creativecommons.org/licenses/by-sa/4.0/) license.



Corresponding Author:

Kahla Sami

Research Center in Industrial Technologies (CRTI)

Cheraga 16014, Algiers, Algeria

Email: samikahla40@yahoo.com

1. INTRODUCTION

Ensuring a consistent output voltage in synchronous generators under dynamic load fluctuations has posed a considerable engineering difficulty, with various investigations documented [1]. Some of these researches are based on an automated voltage regulator (AVR). The AVR is connected to synchronous generators in power production systems to regulate and sustain the generator's terminal voltage at operational levels.

A synchronous generator's exciting system involves sensing the terminal voltage of the generator and comparing it to the reference value. The AVR then adjusts the field voltage of the generator in response to this error signal, regulating the reactive power flow to the load. However, a synchronous generator's terminal voltage magnitude is the primary responsibility of an AVR [2], [3].

Achieving a rapid and reliable reaction from the regulator is difficult because of the power system's complicated performance, which includes factors such nonlinear system characteristics, load change,

different operating points, and the generator field windings' high inductance [4]. In order to make sure the closed loop system responds efficiently to temporary changes in terminal voltage, it is crucial to use a controller to improve the AVR's behavior, resilience, and speed [5], [6].

A decrease in the generator's output voltage is inevitable, resulting from line losses, voltage variations, power outages, and harm to loads and networks. Attaining rapid and consistent voltage management presents a considerable difficulty for the AVR [7]. Consequently, effective control strategies for AVR systems are essential to guarantee the stability of electrical power systems.

Important requirements for AVR systems include stability and the ability to modulate the correct terminal voltage based on load fluctuations; all while avoiding abrupt performance oscillations. Therefore, the AVR system needs careful design to produce a better reaction. In recent years, a number of sophisticated progressive control approaches have been created. The proportional integral derivative (PID) controller is a great main controller for AVR systems because of its simple construction and resilience [8], [9]. Both traditional and cutting-edge approaches to tuning the PID controller settings have shown positive results in the published literature.

In an effort to improve the response of the AVR system, a number of different control strategies have been suggested for the purpose of regulating the generator voltage [10]. Alongside the fractional-order PID controller [11]-[14], fuzzy logic controller (FLC) [15], sliding mode controller (SMC) [16], and the FOPID with optimization techniques [17], [18]. The PID controller is the predominant controller used in AVR systems. This is due to the fact that it is straightforward and easy to construct. As a consequence of this, the enhancement of the efficiency of the AVR system through the development of innovative control strategies continues to be an important and major area of research. More specifically, an improvement should be made to the AVR system's transient reaction.

This paper's principal contributions are detailed:

- A standard PID controller using the sliding mode approach has been designed to maintain the terminal voltage of a synchronous generator at a specified level. The stability of the suggested controller is theoretically confirmed by the Lyapunov theorem.
- The optimization of the suggested controller utilizing the particle swarm optimization (PSO) algorithm.
- A comparative analysis of the proposed controller against PID and PSO-fractional order proportional integral derivative (FOPID) controllers from existing literature to substantiate its efficacy.
- Robustness analysis is used to model uncertainties with other PID and PSO-FOPID controllers documented in the literature.

The organization of this paper is as follows: section 1 presents an overview of the various controllers utilized in the AVR system. Furthermore, section 2 delineates the articulated issue with the regulation of the AVR system. Section 3 offers a comprehensive elucidation of the PSO-PID-SMC approach. Section 4 provides an analysis of the findings achieved and compares the PID-SMC controller in the AVR system utilizing the PSO algorithm with alternative methodologies through several case studies. Ultimately, section 5 encapsulates the conclusions of this research.

2. AUTOMATED VOLTAGE REGULATOR MODEL DESCRIPTION

Synchronous generators display oscillatory behavior around the equilibrium state when subjected to disturbances such as sudden load variations, changes in transmission line properties, fluctuations in turbine output, and analogous conditions. In addition to posing a threat to power system stability, these electromechanical oscillations can limit power transfer capabilities in some cases. Most synchronous generators have an excitation system installed to make the power system more dynamically stable and to guarantee the electricity it delivers is of high quality. A power system stabilizer and an automatic voltage regulator control this system. An AVR's principal role is to keep the magnitude of a synchronous generator's terminal voltage at a constant, predefined value [19]-[21]. Ensuring the stability of the AVR system is essential and crucial to the reliability of the power grid, as stated in [7]. This is why improving the AVR system's stability and transient performance capability via the development of a controller is absolutely necessary.

The standard four-part AVR setup includes a signal source, amplifier, exciter, and generator. Here, we neglect saturation and other nonlinearities in favor of considering a linearized model that accounts for the primary time constant. Here are the respective representations of the transfer functions of these components.

Amplifier output voltage $V_a(s)$ depends on the error voltage $e(s)$. The amplifier model is a first order transfer function defined as (1):

$$G_a(s) = \frac{\Delta V_a(s)}{\Delta e(s)} = \frac{K_a}{1 + \tau_a s} \quad (1)$$

with K_a and τ_a represent respectively the gain and the time constant of the amplifier. The numerical values of the gain k_a and the time constant τ_a are $10 < k_a < 40$ and $0.02 < \tau_a < 0.1$ s. The nominal values of these parameters are $k_a = 40$ and $\tau_a = 0.1$ s.

The field exciter provides a suitable control signal for controlling the voltage across the alternator. Let R_e and L_e represent respectively the resistance and the inductance of the excitation field, then we obtain as (2) and (3):

$$\Delta V_a(s) = R_e \Delta i_e(s) + L_e \frac{d\Delta i_e(s)}{dt} \quad (2)$$

$$\Delta V_a(s) = R_e \Delta i_e(s) + L_e s \Delta i_e(s) \quad (3)$$

Changing the excitation field current Δi_e produces an appropriate field voltage ΔV_e . The variation of the field voltage depends on the variation of the field current.

$$\Delta V_a(s) = K_e \Delta i_e(s) \quad (4)$$

The excitation model is a first order system whose transfer function is (5):

$$G_e(S) = \frac{\Delta V_e(s)}{\Delta V_a(s)} = \frac{K_e}{1 + \tau_e s} \quad (5)$$

with K_e and $\tau_e = \frac{L_e}{R_e}$ represent the constant gain and the time constant of the excitation field. The numerical values of the gain k_e and the time constant τ_e are: $1 < k_e < 10$ and $0.4 < \tau_e < 1.0$ s. The nominal values of the parameters k_e and τ_e are $k_e = 1$ and $\tau_e = 0.4$ s.

Generally, generator the generator field was excited by the field voltage V_e . Let R_f and L_f denote the resistance and reactance of the generator field respectively. At no load (no load applied), the voltage across the generator V_e is proportional to the field current i_f .

$$G_g(S) = \frac{\Delta V_g(s)}{\Delta V_e(s)} = \frac{K_g}{1 + \tau_g s} \quad (6)$$

with K_g and $\tau_g = \frac{L_f}{R_f}$ represent the gain and the time constant of the alternating current (AC) generator. The parameters K_g and τ_g are a function of the variation of loads in the electrical network. The values of these two parameters are such that $0.7 < k_g < 1.0$ and $1.0 < \tau_g < 2.0$ s. Their nominal values are $k_g = 1$ and $\tau_g = 1.0$ s.

The AC generator voltage is measured by the voltage detection device, passed through the rectifier and filter circuit, and then differentiated with the reference voltage V_{ref} to generate a voltage error signal. The main advantage of using a voltage sensor is that it responds quickly to the voltage across the generator.

$$G_s(S) = \frac{\Delta V_s(s)}{\Delta V_g(s)} = \frac{K_s}{1 + \tau_s s} \quad (7)$$

with K_s and τ_s represent the gain and the time constant of the voltage sensor. The values of the gain k_s and the time constant τ_s are $0.9 < k_s < 1.1$ and $0.001 < \tau_s < 0.06$ s. The nominal values of these parameters are $k_s = 1$ and $\tau_s = 0.01$ s. The closed-loop of an AVR system is given in Figure 1.

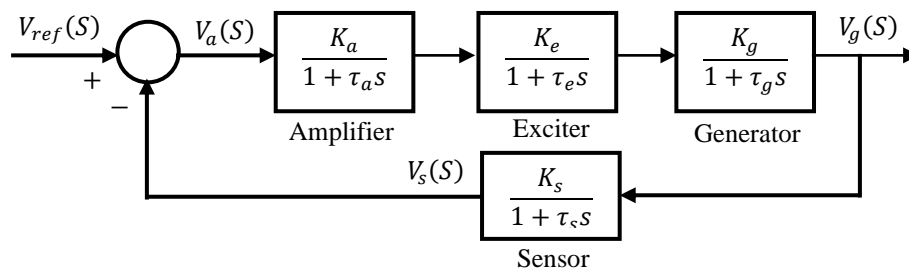


Figure 1. Block diagram of an AVR system (without controller)

The transfer function of the AVR system can be determined by using (1), (5), and (6). It will be used in the design procedure of the PID based on sliding mode control:

$$\frac{V_g(s)}{V_a(s)} = \frac{K_a K_e K_g}{(1 + \tau_a s)(1 + \tau_e s)(1 + \tau_g s)} \quad (8)$$

$$\frac{V_g(s)}{V_a(s)} = \frac{b_1}{a_1 s^3 + a_2 s^2 + a_3 s + 1} \quad (9)$$

where: $a_1 = \tau_a \tau_e \tau_g$, $a_2 = \tau_a \tau_e + \tau_a \tau_g + \tau_e \tau_g$, $a_3 = \tau_a + \tau_e + \tau_g$ and $b_1 = K_a K_e K_g$. Based on the transfer function, we can obtain the following state space model:

$$\begin{cases} \dot{x}_1 = x_2 \\ \dot{x}_2 = x_3 \\ \dot{x}_3 = \frac{1}{a_1} [b_1 u_a - a_2 x_3 - a_3 x_2 - x_1] \end{cases} \quad (10)$$

with: $x_1 = v_g$, $x_2 = \dot{v}_g$, $x_3 = \ddot{v}_g$. v_a is the control signal.

The parameters' values of the AVR system are given in the Table 1 [22]. Figure 2 illustrates the step response of the AVR system without of any controller. The results indicate that the generator's output voltage deviates from the intended reference. The AVR system exhibits significant steady-state inaccuracy, considerable overshoot, prolonged settling time, and oscillatory behavior.

Table 1. Transfer functions and parameter ranges for each AVR component

Component	Transfer function	Range of gains	Range of time constants (s)	Used parameters
Amplifier	$\frac{K_a}{1 + \tau_a s}$	$10 \leq K_a \leq 40$	$0.02 \leq \tau_a \leq 0.1$	$K_a = 10, \tau_a = 0.1$
Exciter	$\frac{K_e}{1 + \tau_e s}$	$1 \leq K_e \leq 10$	$0.4 \leq \tau_e \leq 1$	$K_e = 1, \tau_e = 0.4$
Generator	$\frac{K_g}{1 + \tau_g s}$	$0.7 \leq K_g \leq 1$	$1 \leq \tau_g \leq 2$	$K_g = 1, \tau_g = 1$
Sensor	$\frac{K_s}{1 + \tau_s s}$	$0.9 \leq K_s \leq 1.1$	$0.001 \leq \tau_s \leq 0.06$	$K_s = 1, \tau_s = 0.01$

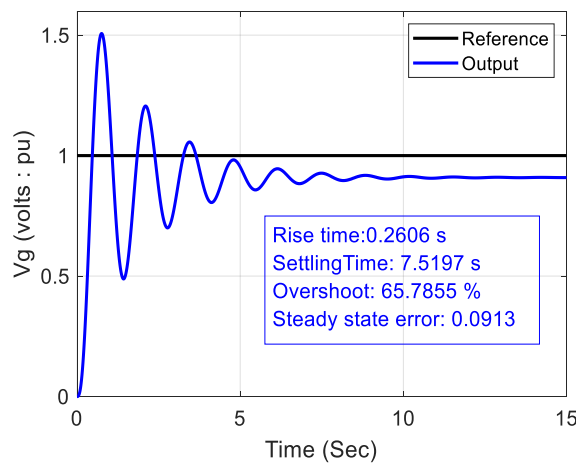


Figure 2. Step response (closed-loop) without controller

The generator's output voltage of the AVR system should be improved. A controller is necessary to eliminate steady-state error and oscillations, thereby reducing the settling time. To achieve the desired response, the particle swarm optimization-proportional integral-derivative (PSO-PID-sliding) mode control is chosen.

3. PARTICLE SWARM OPTIMIZATION OF PROPORTIONAL INTEGRAL-DERIVATIVE BASED ON SLIDING MODE CONTROL

SMC is nonlinear control methodology recognized for its capacity to preserve system's stability in the face of disruptions and fluctuations in system parameters [23]. SMC has been extensively utilized in diverse engineering systems, such as active suspension systems, pneumatic systems, and active magnetic bearing systems, owing to its robustness [24]-[26].

The SMC structure consists of two phases, as illustrated in Figure 3. The initial phase, referred to the reaching phase, compels the system trajectory to transition from a starting condition to the designated sliding surface. The second phase, referred to the sliding phase, occurs after the sliding surface is attained. During this phase, SMC maintains the trajectory of the system on the sliding surface and progresses towards the desired state.

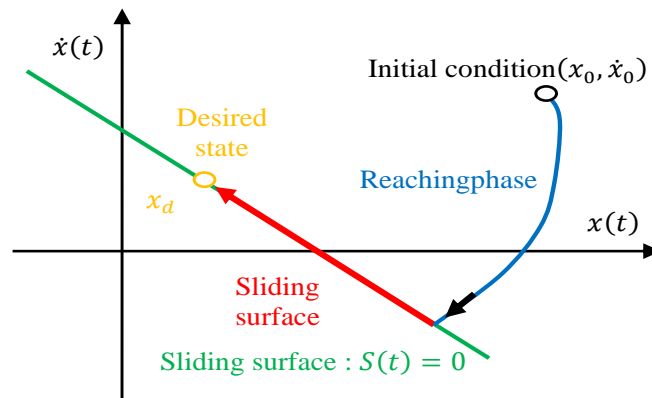


Figure 3. Structure of sliding mode control

The sliding surface is defined with the tracking error, its integral and rate of change:

$$S = K_p e + K_i \int_0^t e d\tau + K_d \dot{e} \quad (11)$$

where K_p , K_i , and K_d are the PID parameters providing flexibility for sliding surface. The tracking error is expressed by (12):

$$e = v_{ref} - v_s = r - x_1 \quad (12)$$

where v_{ref} and v_s are respectively the desired reference and the output system. The expression of SMC control law is defined as (13):

$$u_{SMC} = u_{eq} + u_{sw} \quad (13)$$

where u_{eq} is the equivalent control which refers to the reaching phase when $\dot{S} = 0$, and u_{sw} is the switching control which corresponds to the sliding phase.

The tracking error will remain within the sliding surface and asymptotically converge to the desired point where $S = \dot{S} = \ddot{S} = 0$. The expression for the second derivative of the sliding surface S is (14):

$$\ddot{S} = K_p \ddot{e} + K_i \dot{e} + K_d \ddot{e} \quad (14)$$

The error's third derivative is (15):

$$\ddot{e} = \ddot{r} - \frac{1}{a_1} [b_1 u_a - a_2 x_3 - a_3 x_2 - x_1] \quad (15)$$

Substituting (15) in (14), the expression of \ddot{S} becomes:

$$\ddot{S} = K_p \ddot{e} + K_i \dot{e} + K_d \ddot{r} - \frac{K_d}{a_1} [b_1 u_a - a_2 x_3 - a_3 x_2 - x_1] \quad (16)$$

By introducing $\ddot{S} = 0$ into previous equations, the equivalent control can be obtained as (17):

$$u_{eq} = \frac{1}{b_1} \left[\frac{a_1}{K_d} (K_p \ddot{e} + K_i \dot{e} + K_d \ddot{r}) + a_2 x_3 + a_3 x_2 + x_1 \right] \quad (17)$$

The switching control can be determined as (18):

$$u_{sw} = \eta S + K \text{sign}(\dot{S}) \quad (18)$$

where $K \in R^+$ and $\eta \in R^+$ are respectively the switching gain and exponential coefficient reaching law, and $\text{sign}(\dot{S})$ is the sign function, which is defined as (19):

$$\text{sign}(\dot{S}) = \begin{cases} 1, \dot{S} > 0 \\ 0, \dot{S} = 0 \\ -1, \dot{S} < 0 \end{cases} \quad (19)$$

The SMC control law can be as (20):

$$u_{SMC} = \frac{1}{b_1} \left[\frac{a_1}{K_d} (K_p \ddot{e} + K_i \dot{e} + K_d \ddot{r}) + a_2 x_3 + a_3 x_2 + x_1 \right] + \eta S + K \text{sign}(\dot{S}) \quad (20)$$

The PID-sliding mode control structure for the AVR system is given in Figure 4. It combines the PID regulation with SMC. The PID controller is responsible for ensuring tracking performance and steady-state accuracy, while the SMC ensures robustness against parameter uncertainties and external disturbances in the AVR system.

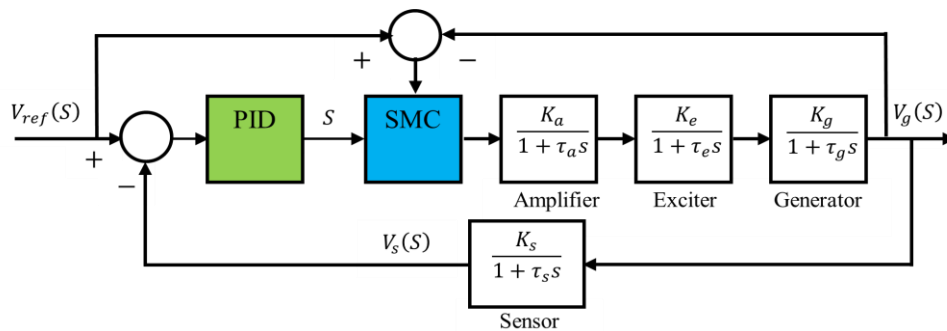


Figure 4. Structure of PSO-PID-sliding mode control of AVR system

The controller's stability has been verified by using Lyapunov's theorem, based on the following Lyapunov function candidate:

$$V(S) = \frac{1}{2} S^2 + \frac{1}{2} \dot{S}^2 \quad (21)$$

with $V(S)$ is a positive definite function ($V(S) > 0, V(0) = 0$).

The derivative of Lyapunov function $V(S)$ with respect of time is given by (22):

$$\dot{V}(S) = S\dot{S} + \dot{S}\ddot{S} \quad (22)$$

Substituting (16) and (20) in (22), we obtain:

$$\dot{V}(S) = S\dot{S} + \dot{S} \left[K_p \ddot{e} + K_i \dot{e} + K_d \ddot{r} - \frac{K_d}{a_1} [b_1 u_{SMC} - a_2 x_3 - a_3 x_2 - x_1] \right] \quad (23)$$

$$\dot{V}(S) = -K\dot{S}sign(\dot{S}) = -K|\dot{S}| < 0 \quad (24)$$

$\dot{V}(S) < 0$ is negative definite. According to Lyapunov theory, the designed controller is asymptotically stable.

Define the tracking error $e = v_{ref} - v_s$, with v_{ref} and v_s are respectively the desired reference and the output system. The sliding surface is defined with the tracking error, its integral and rate of change:

$$S = K_p e + K_i \int_0^t e d\tau + K_d \dot{e} \quad (25)$$

where PID control gains K_p , K_i , and K_d are selected to ensure adequate convergence of the tracking error dynamics (25). The PID-SMC parameters in (25) are optimally tuned through PSO [27]. The optimization aims to minimize the tracking error; which is represented model by (26):

$$\text{Minimize } F = \int_0^t |e| dt \quad (26)$$

$$\text{Subject to } \begin{cases} K_p^{min} \leq K_p \leq K_p^{max} \\ K_i^{min} \leq K_i \leq K_i^{max} \\ K_d^{min} \leq K_d \leq K_d^{max} \end{cases} \quad (27)$$

The proportional gain K_p lie in [8, 24], integral gain K_i is between [16, 144] and derivative gain K_d is bounded in [0.1, 5]. The PSO parameters are selected based on the total number of iterations $N_{iter} = 100$, minimum velocity $v_{min} = 0.1$, maximum velocity $v_{max} = 1$, weight coefficients $c_1/c_2 = 2/2$, respectively. In addition, the convergence criteria is chosen as (28):

$$|F_j - F_{j-1}| \leq \varepsilon \quad (28)$$

Where ε denotes the tolerance of convergence error, which is set to 10^{-2} in this paper; F_j and F_{j-1} denote the fitness function values computed at the J^{th} and the $(j-1)^{th}$ iterations, respectively.

4. SIMULATION AND RESULTS DISCUSSION

The PID, PSO-FOPID controller and PSO-PID-SMC are applied to the AVR system. All simulations and analyses are carried out in MATLAB. The output voltage of the AVR system with PID, PSO-FOPID, and PSO-PID based on sliding mode controller is shown in Figure 5. The obtained result by using PID and PSO-FOPID controller shows that the unit response of the AVR system is more or less fast, with a larger overshoot and some oscillations are observed. However, the result obtained by utilizing the PSO-PID controller base on sliding mode technique exhibits good performances, the overshoot is reduced. We can clearly see that the oscillations have been eliminated.

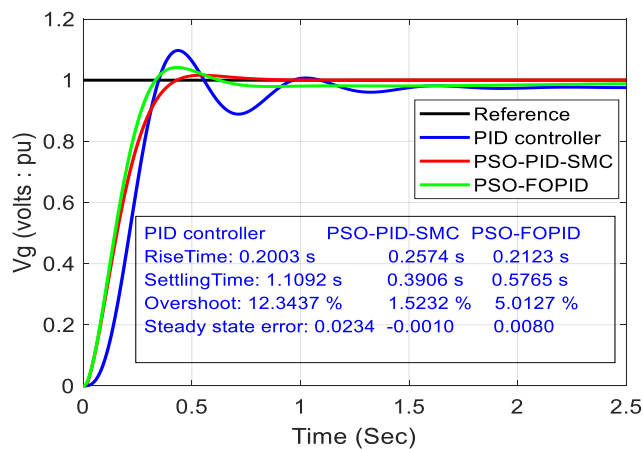


Figure 5. Step response with PID, PSO-FOPID, and PSO-PID-SMC

Table 2 summarizes the performance of the used controllers in term of rise time, settling time, overshoot, steady-state error, mean absolute error, and mean square error. The results clearly indicate the advantage of the PSO-PID-SMC over the other controllers.

Table 2. Performance comparison of the AVR system with PID, PSO-FOPID and PSO-PID-SMC, and without controller

Controllers	Rise time (sec)	Settling time (sec)	Overshoot (%)	Steady state error (p.u)	Mean absolute error	Mean square error
AVR without any controller	0.2606	7.5197	65.7855	0.0913	0.1592	0.538
PID controller	0.2003	1.1092	12.3437	0.0234	0.0991	0.0572
PSO-PID-SMC	0.2574	0.3906	1.5232	0.0010	0.0586	0.0384
PSO-FOPID	0.2123	0.5765	5.0127	0.0080	0.0656	0.0364

4.1. Robustness analysis

All of this points to the fact that, under typical circumstances, the proposed method improves the AVR system's transient characteristics and operates inside a large stability region. But the controller has to make sure the system stays stable even when parameters change and that the transient reaction is effective. The following simulations are run to quantitatively evaluate the system's robustness regarding parameter uncertainty. The system parameters have their temporal constants changed by $\pm 50\%$ in $\pm 25\%$ increments from the nominal value; however, the controller parameters remain fixed. To verify the robustness of the PSO-PID based on sliding mode technique, internal disturbances are applied in the AVR system. The Figure 6 shows the structure of PSO-PID-SMC under disturbances.

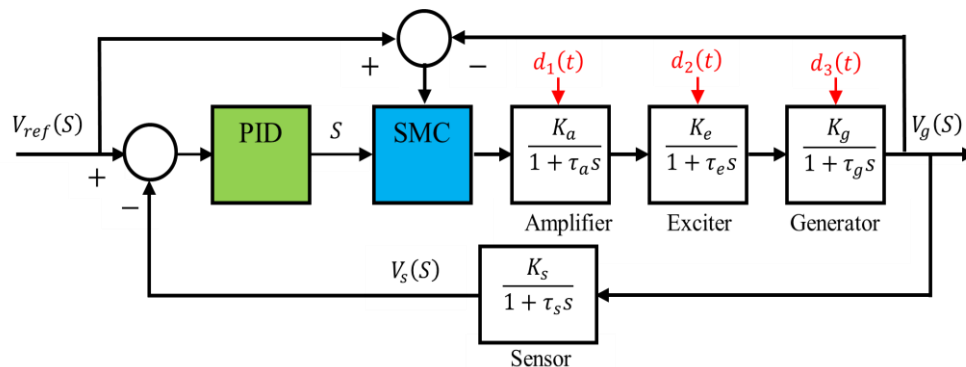


Figure 6. Structure of PSO-PID-sliding mode control of AVR system with parameter uncertainties and disturbance

The proposed controllers' robustness is evaluated under parameter uncertainties injected into the AVR system in the following circumstances:

- Firstly, the amplifier parameters are assumed to be uncertain and varying: $10 \leq K_a \leq 40$ and $0.02 \leq \tau_a \leq 0.1$. The terminal voltage of the AVR system with PID, PSO-PID and PSO-PID based on sliding mode controllers is shown in Figure 7(a).
- It is considered that the parameters of the exciter are uncertain and change: $1 \leq K_e \leq 10$ and $0.4 \leq \tau_e \leq 1$. The terminal voltage with previous designed controllers is shown in Figure 7(b).
- It is assumed that the parameters of the generator are uncertain and change: $0.7 \leq K_g \leq 1$ and $1 \leq \tau_g \leq 2$. The terminal voltage with previous designed controllers is shown in Figure 7(c).

All parameters $K_a, \tau_a, K_e, \tau_e, K_g$ and τ_g are assumed to be uncertain. The unit step response of AVR system with previous designed controllers is shown in Figure 7(d).

Figure 7 and Table 3 demonstrate that the PSO-PID-SMC controller not only achieves effective reference tracking but also improves the system's robustness to model uncertainties. The subsequent table encapsulates the performance metrics of each controller. Table 3 summarizes the performance comparison of the AVR system with PID, PSO-FOPID, and PSO-PID-SMC under parameter uncertainties.

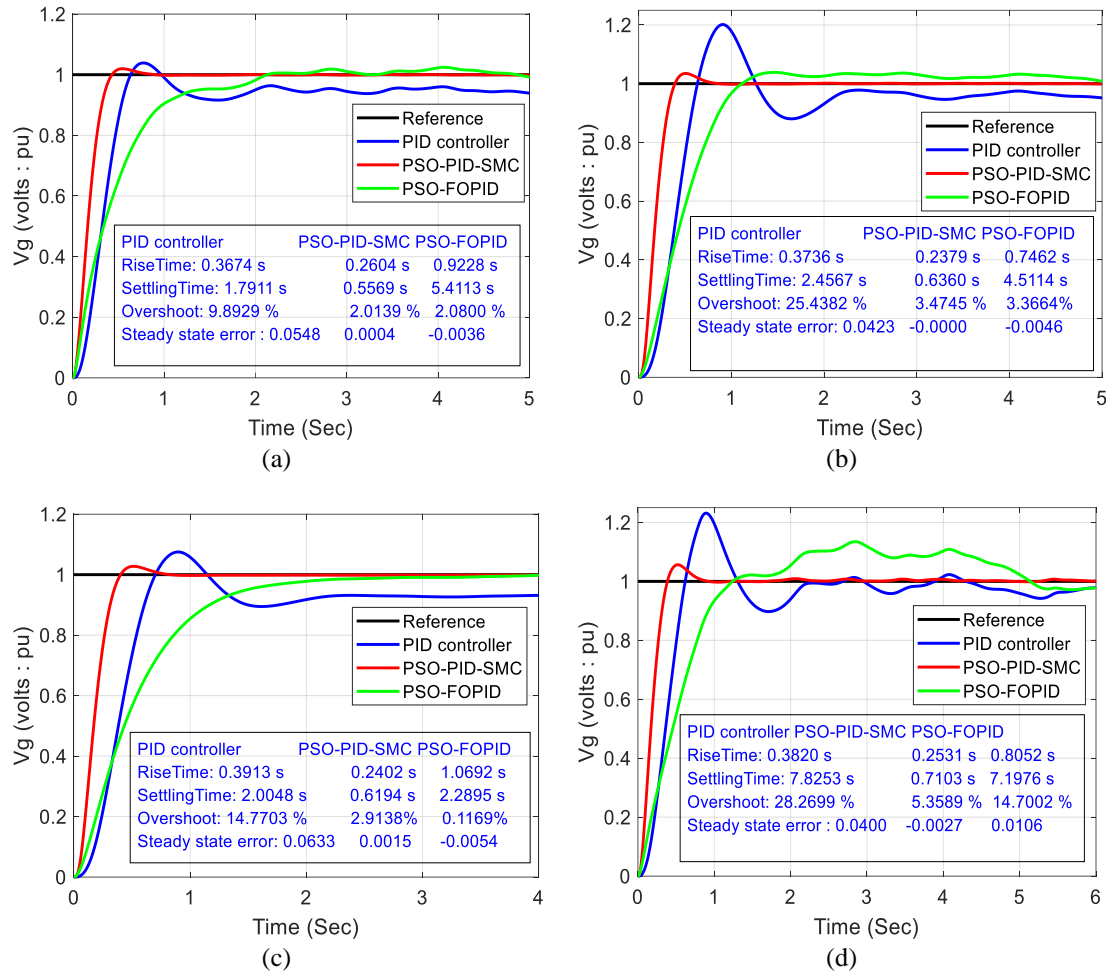


Figure 7. Step response with; (a) for K_a and T_a varying, (b) K_e and T_e varying, (c) K_g and T_g varying, and (d) all parameters varying

Table 3. Performance comparison of the AVR system with PID, PSO-FOPID, and PSO-PID-SMC under parameter uncertainties

Controllers	Rise time (sec)	Settling time (sec)	Overshoot (%)	Steady state error (p.u)	Mean absolute error	Mean square error
Amplifier parameters uncertainties: $10 \leq K_a \leq 40$ and $0.02 \leq \tau_a \leq 0.1$						
PID controller	0.3674	1.7911	9.8929	0.0548	0.0891	0.0331
PSO-PID-SMC	0.2604	0.5569	2.0139	0.0004	0.0233	0.0152
PSO-FOPID	0.9228	5.4113	2.0800	-0.0036	0.0651	0.0308
Exciter parameters uncertainties: $1 \leq K_e \leq 10$ and $0.4 \leq \tau_e \leq 1$						
PID controller	0.3736	2.4567	25.4382	0.0423	0.0953	0.0408
PSO-PID-SMC	0.2379	0.6360	3.4745	-0.0000	0.0243	0.0165
PSO-FOPID	0.7462	4.5114	3.3664	-0.0046	0.0732	0.0389
Generator parameters uncertainties: $0.7 \leq K_g \leq 1$ and $1 \leq \tau_g \leq 2$						
PID controller	0.3913	2.0048	14.7703	0.0633	0.1109	0.0416
PSO-PID-SMC	0.2402	0.6194	2.9138	0.0015	0.0249	0.0164
PSO-FOPID	1.0692	2.2895	0.1169	-0.0054	0.0734	0.0404
All parameters uncertainties						
PID controller	0.3820	7.8253	28.2699	0.0400	0.0826	0.0377
PSO-PID-SMC	0.2531	0.7103	5.3589	-0.0027	0.0270	0.0160
PSO-FOPID	0.8052	7.1976	14.7002	0.0106	0.1046	0.0423

5. CONCLUSION

This study highlights the crucial role of an AVR in maintaining the voltage of the synchronous generator and protecting equipment from potential damage. It emphasizes the importance of key parameters

including; voltage regulation, response time, system stability, and efficiency performance under varying parameters: K_a , τ_a , K_e , τ_e , K_g , and τ_g . Due to the unsatisfactory performance of the uncontrolled AVR system. Characterized by long settling time, significant oscillations and excessive overshoots, the use of a robust and appropriate controller becomes imperative. This research proposes a PSO optimization methodology for tuning the parameters of PID-SMC and FOPID controllers in AVR systems. The results demonstrate that no controller is superior to its counterpart across all potential design requirements. The PSO-PID based on SMC has superior performance in achieving the conflicting goals of settling time, overshoot, and steady-state error compared to the PSO-FOPID and PID controllers. Nonetheless, for the rising time target, the PID controller surpasses both the PSO-based PID-SMC and PSO-FOPID controllers, respectively. The suggested controller's performance is assessed using set-point tracking and modifications in parameters. In all test scenarios, the suggested controller demonstrated exceptional efficiency and provided steady and robust responses.

ACKNOWLEDGMENTS

The authors express their gratitude to The Directorate-General for Scientific Research and Technological Development of Algeria for its support.

FUNDING INFORMATION

Authors state no funding involved.

AUTHOR CONTRIBUTIONS STATEMENT

This journal uses the Contributor Roles Taxonomy (CRediT) to recognize individual author contributions, reduce authorship disputes, and facilitate collaboration.

Name of Author	C	M	So	Va	Fo	I	R	D	O	E	Vi	Su	P	Fu
Lemita Abdallah	✓	✓	✓	✓	✓	✓	✓	✓	✓	✓	✓	✓	✓	✓
Lemita Ines		✓			✓			✓		✓	✓			✓
Kahla Sami		✓	✓		✓			✓		✓	✓		✓	✓

C : Conceptualization

M : Methodology

So : Software

Va : Validation

Fo : Formal analysis

I : Investigation

R : Resources

D : Data Curation

O : Writing -Original Draft

E : Writing - Review &Editing

Vi : Visualization

Su : Supervision

P : Project administration

Fu : Funding acquisition

CONFLICT OF INTEREST STATEMENT

The authors declare that they have no conflicts of interest.

INFORMED CONSENT

All individuals who participated in this paper provided informed consent.

ETHICAL APPROVAL

This paper does not involve any people participant or animals studies.

DATA AVAILABILITY




This paper does not involve any data that require availability admission.

REFERENCES




- [1] X. Meng, P. Zhang, Y. Xu, and H. Xie, "Construction of decision tree based on C4.5 algorithm for online voltage stability assessment," *International Journal of Electrical Power and Energy Systems*, vol. 118, pp. 1-8, 2020, doi: 10.1016/j.ijepes.2019.105793.

- [2] M. Xie, M. M. Gulzar, H. Tehreem, M. Y. Javed, and S. T. H. Rizvi, "Automatic voltage regulation of grid connected photovoltaic system using lyapunov based sliding mode controller: A finite — time approach," *International Journal of Control, Automation and Systems*, vol. 18, no. 6, pp. 1550–1560, 2020, doi: 10.1007/s12555-019-0563-x.
- [3] M. A. Nasr, S. Nikkhah, G. B. Gharehpetian, E. N. Azadani, and S. H. Hosseini, "A multi-objective voltage stability constrained energy management system for isolated microgrids," *International Journal of Electrical Power and Energy Systems*, vol. 117, pp. 1–11, 2020, doi: 10.1016/j.ijepes.2019.105646.
- [4] M. Kalidasan, T. G. Sekar, and T. Mohanasundaram, "Power loss reduction and voltage profile enhancement by reconfiguration of radial distribution system with hybrid optimization method," *Thermal Science and Engineering Progress*, vol. 57, p. 103105, 2025, doi: 10.1016/j.tsep.2024.103105.
- [5] M. M. Kumar, A. A. Rani, and V. Sundaravazhuthi, "A computational algorithm based on biogeography-based optimization method for computing power system security constraints with multi FACTS devices," *Computational Intelligence*, vol. 36, no. 4, pp. 1493–1511, 2020, doi: 10.1111/coin.12282.
- [6] M. Ş. Üney and N. Çetinkaya, "New metaheuristic algorithms for reactive power optimization," *Tehnicki Vjesnik*, vol. 26, no. 5, pp. 1427–1433, 2019, doi: 10.17559/TV-20181205153116.
- [7] S. Ekinici and B. Hekimoglu, "Improved kidney-inspired algorithm approach for tuning of PID controller in AVR system," *IEEE Access*, vol. 7, pp. 39935–39947, 2019, doi: 10.1109/ACCESS.2019.2906980.
- [8] Z. L. Gaing, "A particle swarm optimization approach for optimum design of PID controller in AVR system," *IEEE Transactions on Energy Conversion*, vol. 19, no. 2, pp. 384–391, 2004, doi: 10.1109/TEC.2003.821821.
- [9] Z. Bingul and O. Karahan, "A novel performance criterion approach to optimum design of PID controller using cuckoo search algorithm for AVR system," *Journal of the Franklin Institute*, vol. 355, no. 13, pp. 5534–5559, 2018, doi: 10.1016/j.jfranklin.2018.05.056.
- [10] B. Hekimoğlu, "Sine-cosine algorithm-based optimization for automatic voltage regulator system," *Transactions of the Institute of Measurement and Control*, vol. 41, no. 6, pp. 1761–1771, 2019, doi: 10.1177/0142331218811453.
- [11] Y. Tang, M. Cui, C. Hua, L. Li, and Y. Yang, "Optimum design of fractional order PI λ D μ controller for AVR system using chaotic ant swarm," *Expert Systems with Applications*, vol. 39, no. 8, pp. 6887–6896, 2012, doi: 10.1016/j.eswa.2012.01.007.
- [12] G. Q. Zeng, J. Chen, Y. X. Dai, L. M. Li, C. W. Zheng, and M. R. Chen, "Design of fractional order PID controller for automatic regulator voltage system based on multi-objective extremal optimization," *Neurocomputing*, vol. 160, pp. 173–184, 2015, doi: 10.1016/j.neucom.2015.02.051.
- [13] I. Pan and S. Das, "Frequency domain design of fractional order PID controller for AVR system using chaotic multi-objective optimization," *International Journal of Electrical Power and Energy Systems*, vol. 51, pp. 106–118, 2013, doi: 10.1016/j.ijepes.2013.02.021.
- [14] M. S. Ayas and E. Sahin, "FOPID controller with fractional filter for an automatic voltage regulator," *Computers and Electrical Engineering*, vol. 90, pp. 1–12, 2021, doi: 10.1016/j.compeleceng.2020.106895.
- [15] T. Gupta and D. K. Sambariya, "Optimal design of fuzzy logic controller for automatic voltage regulator," in *IEEE International Conference on Information, Communication, Instrumentation and Control, ICICIC 2017*, Aug. 2017, pp. 1–6, doi: 10.1109/ICOMICON.2017.8279140.
- [16] R. L. A. Ribeiro, C. M. S. Neto, F. B. Costa, T. O. A. Rocha, and R. L. Barreto, "A sliding-mode voltage regulator for salient pole synchronous generator," *Electric Power Systems Research*, vol. 129, pp. 178–184, 2015, doi: 10.1016/j.epsr.2015.07.016.
- [17] I. Moschos and C. Parissis, "A novel optimal PI λ DND2N2 controller using coyote optimization algorithm for an AVR system," *Engineering Science and Technology, an International Journal*, vol. 26, pp. 1–12, 2022, doi: 10.1016/j.jestech.2021.04.010.
- [18] B. Bourouba, S. Ladaci, and H. Schulte, "Optimal design of fractional order PI λ D μ controller for an AVR system using ant lion optimizer," *IFAC-PapersOnLine*, vol. 52, no. 13, pp. 200–205, 2019, doi: 10.1016/j.ifacol.2019.11.304.
- [19] M. E. O. Quisbert, M. A. D. Mermoud, F. Milla, R. C. Linares, and G. Lefranc, "Optimal fractional order adaptive controllers for AVR applications," *Electrical Engineering*, vol. 100, no. 1, pp. 267–283, 2018, doi: 10.1007/s00202-016-0502-2.
- [20] Z. L. Gaing, "A particle swarm optimization approach for optimum design of PID controller in AVR system," *IEEE Transactions on Energy Conversion*, vol. 19, no. 2, pp. 384–391, 2004, doi: 10.1109/TEC.2003.821821.
- [21] M. A. Sahib, "A novel optimal PID plus second order derivative controller for AVR system," *Engineering Science and Technology, an International Journal*, vol. 18, no. 2, pp. 194–206, 2015, doi: 10.1016/j.jestech.2014.11.006.
- [22] M. M. Zirkohi, "An efficient optimal fractional emotional intelligent controller for an AVR system in power systems," *Journal of AI and Data Mining*, vol. 7, no. 1, pp. 193–202, 2019, doi: 10.22044/JADM.2018.6797.1798.
- [23] C. Edwards and S. Spurgeon, "Sliding Mode Control Theory and Applications," *CRC Press*, Taylor & Francis Ltd 1998.
- [24] Y. M. Sam and J. H. S. B. Osman, "Modeling and control of the active suspension system using proportional integral sliding mode approach," *Asian Journal of Control*, vol. 7, no. 2, pp. 91–98, 2005, doi: 10.1111/j.1934-6093.2005.tb00378.x.
- [25] Y. T. Liu, T. T. Kung, K. M. Chang, and S. Y. Chen, "Observer-based adaptive sliding mode control for pneumatic servo system," *Precision Engineering*, vol. 37, no. 3, pp. 522–530, 2013, doi: 10.1016/j.precisioneng.2012.12.003.
- [26] A. R. Husain, M. N. Ahmad, A. Halim, and M. Yatim, "Chattering-free sliding mode control for an active magnetic bearing system," *International Journal of Mechanical, Aerospace, Industrial, Mechatronics and Manufacturing Engineering*, vol. 2, no. 3, pp. 300–306, 2008.
- [27] X. Li, Y. Wang, N. Li, M. Han, Y. Tang, and F. Liu, "Optimal fractional order PID controller design for automatic voltage regulator system based on reference model using particle swarm optimization," *International Journal of Machine Learning and Cybernetics*, vol. 8, no. 5, pp. 1595–1605, 2017, doi: 10.1007/s13042-016-0530-2.




BIOGRAPHIES OF AUTHORS

Lemita Abdallah    is Professor on Department of Electrical Engineering, Faculty of Sciences and Technology, University of Echahid Cheikh Larbi Tebessi, Tebessa, Algeria. He obtained B.Sc. degree in Electronic Engineering in 2009 from the University of Cheikh Larbi Tebessi, Tebessa, Algeria. He also received his degree of Magister in electronic in 2014 from the University Ferhat Abbas of Setif 1, Algeria. He holds a Ph.D. degree in electronic in 2021 from the University Ferhat Abbas of Setif 1, Algeria. His research areas are electronic, automatic, and control system. He has supervised 6 masters' students. He can be contacted at email: abdallah.lemita@univ-tebessa.dz.



Lemita Ines    is a Ph.D. student. She obtained Master degree in Electrical Engineering in 2021 from the University of Echahid Cheikh Larbi Tebessi, Tebessa, Algeria. She is currently a Ph.D. student at the University of Mohamed Cherif Messaadia, Souk Ahras, Algeria. His research areas are electrical engineering and network. She can be contacted at email: i.lemita@univ-soukahras.dz.



Kahla Sami    received the B.Sc. and Magister degrees in automatic from Tebessa University, Algeria in 2009 and 2013 respectively and the Ph.D. degree in electrical engineering from the University of Guelma, Algeria in 2018, and the Habilitation degree from 8 Mei 1945 Guelma University, Algeria in 2021. He joined the Research Center in Industrial Technologies (CRTI), Algiers, Algeria in 2014. He is currently working as a Senior Researcher 'A'. His research interests include power energy conversion systems, fuzzy logic control (FLC), metaheuristic optimization algorithms, and power electronics. He can be contacted at email: samikahla40@yahoo.com.